Modeling indoor propagation using an indirect hybrid method combining the UTD and the FDTD methods

Sébastien Reynaud[1], Christophe Guiffaut[1], Alain Reineix[1], Rodolphe Vauzelle[2]

[1]University of Limoges, IRCOM, UMR CNRS 6615, 123 avenue Albert Thomas, 87000 Limoges
[2]University of Poitiers, SIC, FRE CNRS 2731, Boulevard Marie et Pierre Curie, 86360 Chasseneuil-du-Poitou
E-Mail : sebastien.reynaud@unilim.fr

***Abstract*— Classical theories such as the Uniform Theory of Diffraction (UTD) use analytical expressions for diffraction coefficients [1]. These methods are convenient for canonical problems for objects much greater than the wavelength and enable to rise in frequency. For more complex and smaller scattering structures, the rigorous methods like the Finite Difference Time Domain method (FDTD) is more adapted [2]. In this paper, we present an original approach, combining the advantages of these two complementary methods. So, the propagation channel can be accurately characterised.**

I. Introduction

Nowadays, an increasing interest is devoted to wide-band applications like Wireless Local Area Networks (WLANs), because the present multimedia services require more high bit rate and thus large bandwidth. Recently, ray tracing techniques (RT), associated to the UTD [1], have emerged as the dominant techniques to predict the wide-band channel behaviour. Indeed, these asymptotic methods are fast and not limited in frequency. However, dealing with INDOOR propagation, this classical approach is not sufficient to model object of wavelength size or with complex forms. For these structures, rigorous methods like the FDTD, consisting in solving Maxwell's equations in discrete time domain, are well-suitable. In this paper, we present a hybrid method, combining the advantages of the UTD and the FDTD methods, in order to enhance the propagation channel's modelling. On the one hand, the RT technique is used to model the wave propagation in rooms, corridors, and buildings including large objects : the diffracted field is computed using the uniform coefficient diffraction of Kouyoumjian and Pathak [3], as well as the Fresnel's transition function at the shadow boundaries; the total field is deduced by superposition of the components existing in the different regions. On the other hand, the FDTD method is chosen to calculate a scattering matrix of smaller and more complex structures. This matrix constitutes the interface between the object and RT method. In this paper, we first present a detailed description of the hybrid method. Then, in order to validate the hybrid method, we compare the results obtained using UTD and FDTD for the simple case of a finite metallic sheet. After that, we study a structure for which the RT technique is not applicable : a square metallic structure. In this case, we compare the results provided by the FDTD and the hybrid method. Finally, we present the results obtained for two more complex structures and we conclude on the perspectives of this study.

II. Description of the method

Two steps are needed for the hybrid method (Fig. 1) :

1) The FDTD method is used for the determination of the scattering matrix of a studied structure.
2) The scattering matrix is included into an asymptotic approach as a generalized diffraction coefficient.

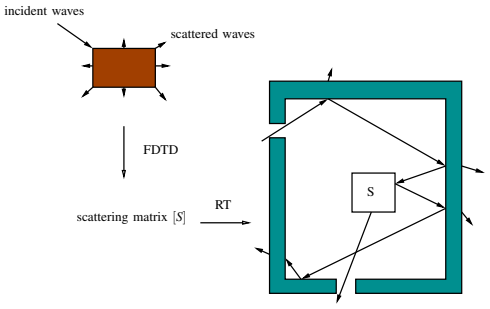

Fig. 1. Principle of the hybrid method

A. determination of the scattering matrix

The scattering matrix is computed by the FDTD method. Fig. 2 shows the different regions in the computational volume of the FDTD method.

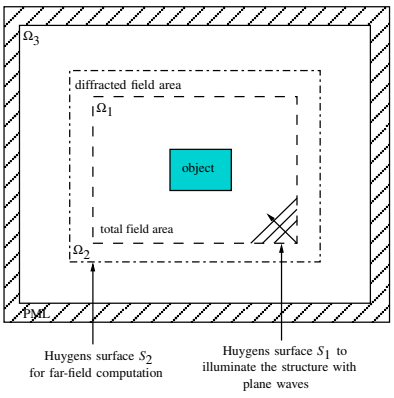

Fig. 2. FDTD computation

We first illuminate the object with a pulsed plane wave. Following the principle of Huygens, a first surface is placed around the structure : the equivalent currents existing on this surface generate an incident field inside this Huygens box, in the region Ω_1. After interaction between the incident

waves and the structure, outside S_1 in the region Ω_2, the computed field gives the field scattered by the structure. Thus, by means of a Fourier transformation, we get the diffracted field in the near-field region in the frequency domain. The main hypothesis of application of the hybrid method is to get far-field conditions of propagation. To play this part, we place another Huygens box S_2 around the first one : the equivalent electrical and magnetical currents radiate outside this second surface and, thanks to a near-to-far field transformation, we obtain the diffracted far field. Knowing the incident field at the phase centre P chosen for the near-to-far field transformation, we deduce a scattering matrix in frequency domain for a given frequency and angle of illumination. This scattering matrix gathers the diffraction coefficients for various angles of observation :

$$D(\phi_i,\phi_o,f) = \frac{E_{far}(\phi_i,\phi_o,f)}{E_{inc}^{planewave}(P)} \quad (1)$$

In equation 1, ϕ_i and ϕ_o are the angles of incidence and observation calculated in relation to the lines $\phi_i = 0$ and $\phi_o = 0$ respectively (Fig. 3). $E_{far}(\phi_i,\phi_o,f)$ is the far-field obtained in the direction ϕ_o at a normalized distance of 1 meter and $E_{inc}(P)$ is the incident field computed with plane waves at the phase centre P of the studied structure.

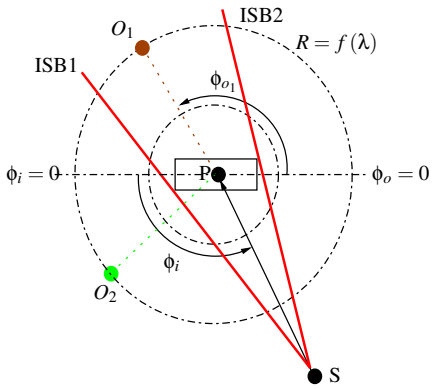

Fig. 3. Principle of the scattering matrix computation

B. rectification of the scattering matrix

The computation of the scattering matrix is based on the principle of Huygens. According to this principle, the incident field is confined inside the region Ω_1 (Fig. 2); in the region Ω_2, the computed field corresponds to the total field minus the incident field. The physical field will consequently be false when the observation's point is located inside the shadowed region. As a matter of fact, we have to compensate this error by adding a correcting component to the diffraction coefficient for the directions of interest (i.e in the shadowed region). This component deals with the incident field at the observation's point. It clearly appears that this factor will depend on the emission's point, since the shadowed region change with the position of the source. More precisely, we found that this correcting component E_{cor} is equal to :

$$E_{cor}\left(r,s'\right) = E_{inc}^{planewave}(P)\,\frac{\psi(r)}{\psi\left(s'\right)} \quad (2)$$

where r, s' are the distances respectively from the transmitter to the receiver and from the transmitter to the phase centre. $\psi(r)$ and $\psi\left(s'\right)$ are the 3D-Green functions equal to $\psi(R) = \frac{e^{-jkR}}{R}$ with k the wave vector.

In all the simulations presented below, we consider a 2-D propagation (xOy plane). The represented field is observed over circles centred on the structure with various radius (Fig. 3). As a consequence, we will have to use the 2D-Green functions equal to $\psi_{2D}(R) = \psi(R)\,F_{2D}$ where $F_{2D} = \sqrt{\left(\frac{2\pi}{ik}\right)}\frac{1}{\Delta z}$ with Δz the computational spatial step in z direction of the FDTD method.

In the Ray Tracing code, the object will now be replaced by its scattering matrix and viewed as a simple point of diffraction.

III. Main results

In order to avoid normalisation's problems, we use a perfect isotropic current source with a gaussian envelope modulated by a sinusoïde function for the three methods. We use a TM polarized wave of center frequency $2GHz$. For the results presented below, we compute the scattering matrix using a FDTD code with Berenger perfectly matched layer as (PML) absorbing boundary conditions [4]. In the FDTD code, we use square grid cells of side length of resolution $\frac{\lambda_0}{60}$ to minimize numerical errors, where λ_0 is the wavelength at $2GHz$; the source is placed at distance 20 λ from the structure. Four cases are studied : the first one corresponds to a simple finite metallic sheet; the others are smaller and more complex structures for which the UTD is not applicable.

A. The finite metallic sheet

We simulate the diffraction by a λ_0 length metallic sheet with a normal incident wave. Fig. 4 represents the normalized total field observed at λ_0 around the structure.

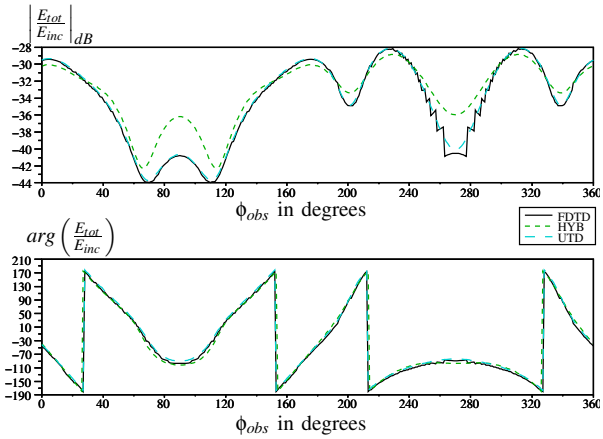

Fig. 4. Comparison of the FDTD, UTD and hybrid results for the normalized total field at distance λ_0 around the λ_0 length metallic sheet

We can see that the hybrid method provides false results in front of and behind the structure. In fact, we observe the field in the near-field region : indeed, the diffraction by a metallic sheet is quite similar to the diffraction by an aperture for which the far-field area is related to the length d of the aperture and the wavelength by $\frac{2d^2}{\lambda_0}$. For instance, the far-field region would be at $2\lambda_0$ because the length of the metallic sheet is λ_0. Fig. 5 shows the magnitude of the normalized diffracted field from the λ_0 length metallic sheet computed on a line between the structure and the source (normal incidence).

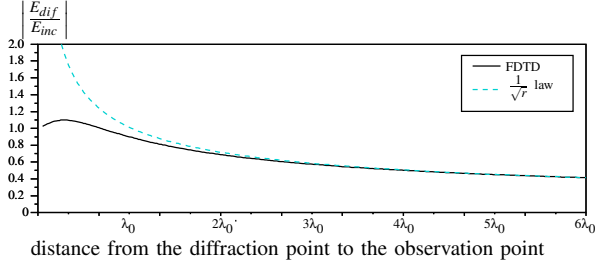

Fig. 5. Scattered field for the λ_0 length metallic sheet, according to the distance

It highlights that the results obtained with the hybrid method - which follows a $\frac{1}{\sqrt{r}}$ law - well suit those computed by FDTD after a distance of $2\lambda_0$. Fig. 6 illustrates this remark since there is a good agreement between the three methods at distance $5\lambda_0$.

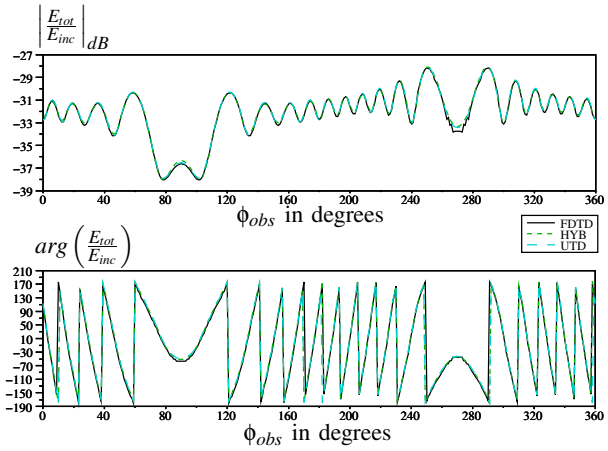

Fig. 6. Comparison of the FDTD, UTD and hybrid results for the normalized total field at distance $5\lambda_0$ around the λ_0 length metallic sheet

B. The square metallic structure

The studied square metallic structure is side length $\frac{\lambda_0}{2}$: in this case, the RT technique is not applicable because the dimensions of the structure are about the wavelength. So, the hybrid method is interesting. Following the procedure used for the metallic sheet, we compare the hybrid and FDTD results for the square metallic structure with side length $\frac{\lambda_0}{2}$. Now, the angle of illuminaton is 45°. We observe the normalized total field on a circle with radius $3\lambda_0$ (Fig. 7).

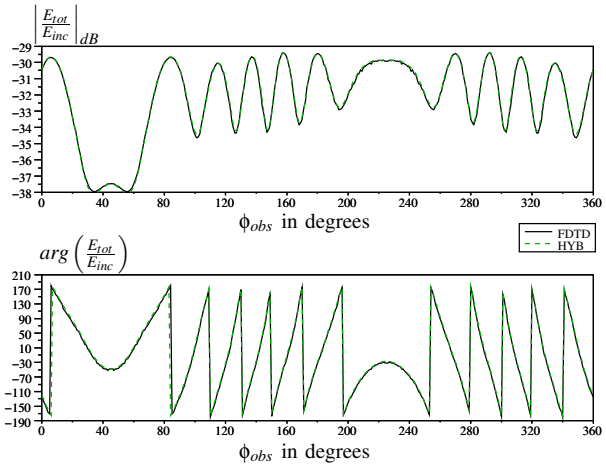

Fig. 7. Comparison of the FDTD and hybrid results for the normalized total field at distance $3\lambda_0$ around the $\frac{\lambda_0}{2}$ square metallic structure

There is a good agreement between the hybrid and the FDTD results. As for the finite metallic sheet, we can see on Fig. 7. that when the points of observation are in the far-field region, the two methods give similar results. However, we encountered differences between the two methods when the distance of observation is smaller than $3\lambda_0$: the hybrid method gives results quite different to those of the FDTD, probably because the far-field conditions of propagation are not respected under a distance $3\lambda_0$.

C. Two more complex structures

The first studied structure is represented on Fig. 8. In order to see the impact of the dimensions of a given structure, we have taken the same conditions of simulation for two similar structures (L metallic structure). The variable parameter is a scale factor on the dimensions of the structure (here a scale factor equal to 4). The angle of incidence is still 45°.

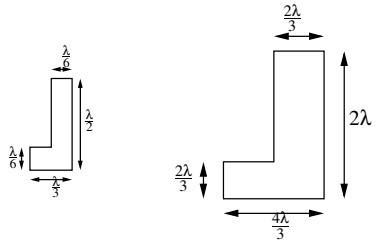

Fig. 8. The two L-structures

The results for the smaller L metallic structure are represented on Fig. 9. We observe the normalized total field at distance $3\lambda_0$ around the structure. There is a good agreement between the hybrid method and the FDTD method, even in the shadowed region. Notice that at distance $2\lambda_0$, the results (not presented here) are a little bit false in the shadowed region. It supposes that the far-field conditions for this studied structure are globally respected at a distance of $3\lambda_0$ from the phase centre.

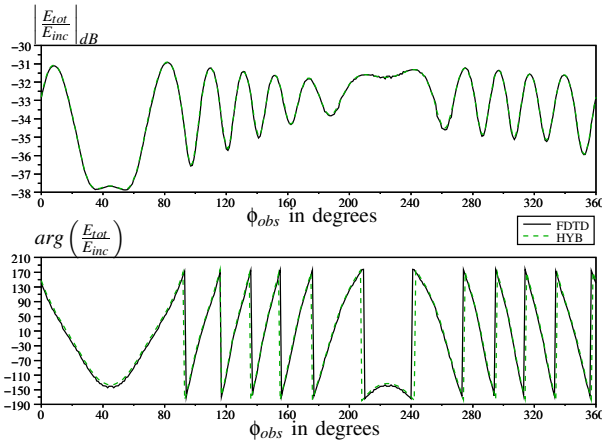

Fig. 9. Comparison of the FDTD and hybrid results for the normalized total field at distance $3\lambda_0$ around the smaller L structure

For the larger L metallic structure, Fig. 10 shows the total field observed at distance $3\lambda_0$ around the structure. The results provided by the hybrid method are far from the FDTD results : the far-field conditions are not respected in this configuration.

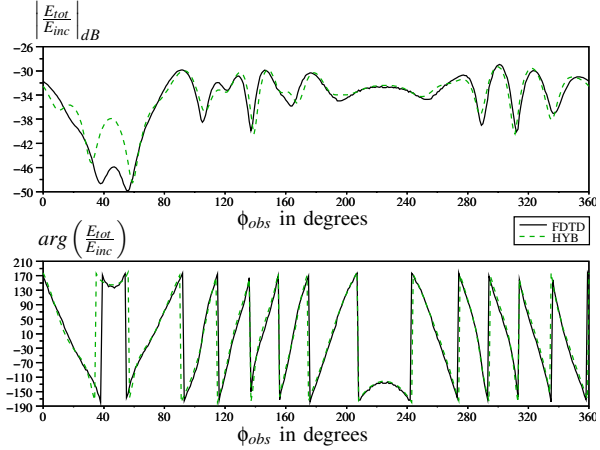

Fig. 10. Comparison of the FDTD and hybrid results for the normalized total field at distance $3\lambda_0$ around the larger L structure

Fig. 11 shows the total field observed at distance $12\lambda_0$ for the same structure. The results provided by the hybrid method well suits the FDTD ones, except in the shadowed region. In fact, in this region, there are no dominant components and the field is a combination of multiple diffractions so that the wave can be considered as plane wave further than in the others regions.

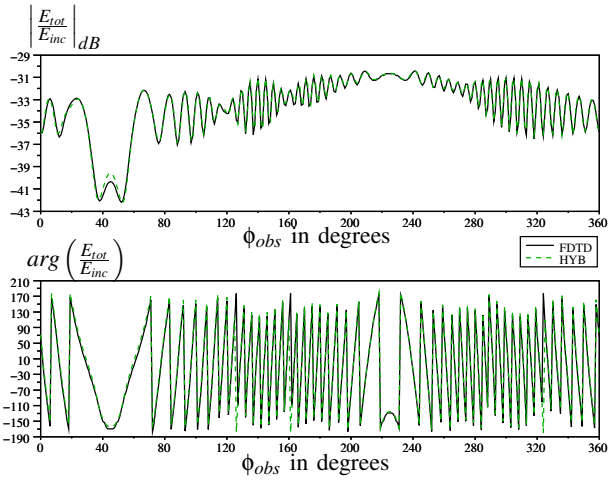

Fig. 11. Comparison of the FDTD and hybrid results for the normalized total field at distance $12\lambda_0$ around the larger L structure

From the two simulations above, we can conclude that for a given structure, the far-field conditions depend on the direction of observation and on the dimensions of the structure. It seems that in the shadowed region the wave can be considered as a plane-wave later than in the others directions. Concerning the dimensions of the structure, we can conclude that the scale factor seems to be respected since in the first case, the far-field conditions were globally obtained at distance $3\lambda_0$ whereas for the second one, they are respected after a distance $12\lambda_0$.

To see the influence of the form of the object we took the exemple of a U metallic structure with dimensions about the smaller L metallic structure. The normalized total field is observed at $3\lambda_0$ in order to compare with the results obtained for the smaller L metallic structure.

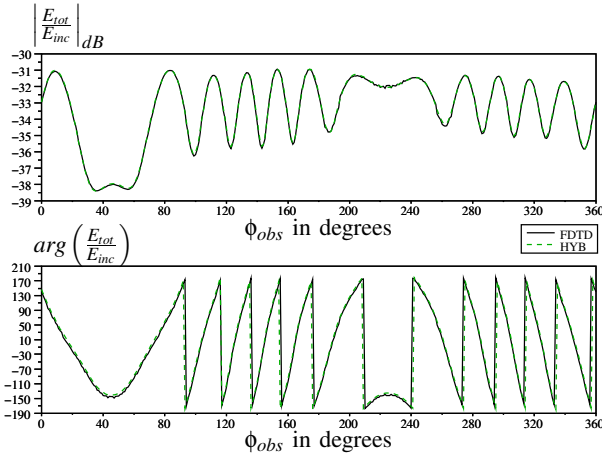

Fig. 12. Comparison of the FDTD and hybrid results for the normalized total field at distance $3\lambda_0$ around the U structure

The results presented on Fig. 12 highlights that the hybrid method is suitable at this distance. It seems that the far-field conditions depend more on the overall dimension of the structure than on the form of the structure.

IV. Conclusion

In this paper, we presented an original approach combining the FDTD and the UTD methods to obtain the field diffracted in the far-field region for scatterers in 2-D. We have illustrated the accuracy of this method for a finite 2-D metallic sheet for selected key observation regions, as well as for more complex structures. We found that the accuracy of the hybrid method depends on the form and the dimensions of the structures. In fact, this method aims to compute scattered fields by generic structures with arbitrary wedge angles. Further, we want to extend this approach to the 3-D propagation modelling by calculating a library of diffraction coefficients for a variety of 3-D complex structures. A study will be done around parameters such as the dimensions, the form or the material of the structures, in order to determine the domain where the hybrid method computes suitable fields. Globally, for wireless indoor applications, our goal with the presented hybrid method is to evaluate the influence of small and complex structures on the channel modelling.

References

[1] D. McNamara, C. Pistorius, and J. Malherbe, *Introduction to the Uniform Geometrical Theory of Diffraction*. Artech House, Inc., 1990.

[2] A. Taflove, *Computational electrodynamics, The finite difference time domain method*. Artech House, Inc., 1995.

[3] R. Kouyoumjian and P. Pathak, "A uniform geometrical theory of diffraction for an edge in a perfectly conducting surface," in *Proc. IEEE*, vol. 62, Novembre 1974, pp. 1448–1461.

[4] J. Berenger, "A perfectly matched layer for the absorption of electromagnetic waves," in *J. Computational Physics*, vol. 114, 1994, pp. 185–200.